



This is a repository copy of *Non-invasive measurement of lubricating oil viscosity using an ultrasonic continuously repeated chirp shear wave*.

White Rose Research Online URL for this paper:

<https://eprints.whiterose.ac.uk/136085/>

Version: Published Version

Article:

Manfredi, O.F., Mills, R.S., Schirru, M.M. et al. (1 more author) (2019) Non-invasive measurement of lubricating oil viscosity using an ultrasonic continuously repeated chirp shear wave. *Ultrasonics*, 94. pp. 332-339. ISSN 0041-624X

<https://doi.org/10.1016/j.ultras.2018.08.002>

Reuse

This article is distributed under the terms of the Creative Commons Attribution (CC BY) licence. This licence allows you to distribute, remix, tweak, and build upon the work, even commercially, as long as you credit the authors for the original work. More information and the full terms of the licence here:

<https://creativecommons.org/licenses/>

Takedown

If you consider content in White Rose Research Online to be in breach of UK law, please notify us by emailing eprints@whiterose.ac.uk including the URL of the record and the reason for the withdrawal request.



eprints@whiterose.ac.uk
<https://eprints.whiterose.ac.uk/>



Non-invasive measurement of lubricating oil viscosity using an ultrasonic continuously repeated chirp shear wave

O.F. Manfredi*, R.S. Mills, M.M. Schirru, R.S. Dwyer-Joyce

Leonardo Centre for Tribology, University of Sheffield, Sheffield S1 3JD, UK



ARTICLE INFO

Keywords:
Ultrasonic viscometry
Newtonian
Standing wave, Ultrasound
Viscosity measurement

ABSTRACT

The ability to monitor the viscosity of lubricating oils within metallic products is of interest to many industries, these being the automotive, aerospace and food industries to name a few. Acoustic mismatch at the metallic-liquid interface restricts ultrasonic signal transmission and so limits applicability and sensitivity of the technique. In this work, we propose the use of a continuously repeated chirp (CRC) shear wave to amplify the measurable acoustic response to liquid viscosity. The technique enables multiple reflections to superimpose inside the component and form a quasi-static standing wave whose amplitude spectrum depends on the condition at the solid-liquid boundary. Bare element shear ultrasonic transducers of 5 MHz resonant frequency were bonded to the lower surface of an aluminium plate in a pitch-catch arrangement to measure liquid in contact with the upper surface. Transducers were pulsed using a continuously repeated frequency sweep, from 0.5 to 9.5 MHz over 10 ms. The amplitude spectrum of the resulting standing wave was observed for a series of standard viscosity oils, which served as a calibration procedure, from which the standing wave reflection coefficient (S), was obtained. Measurements of 17 blended oils ranging in viscosity from 1080 to 6.7 mPa s were made. The technique was also evaluated with the addition of a polyimide matching layer (ML) between the metallic and liquid interface. Ultrasonic viscosity measurement values were then compared to measurements made using a conventional laboratory viscometer. The CRC method was found to significantly improve the sensitivity of viscosity measurement at a metal-liquid interface when compared to a single frequency burst with the benefit of low cost signal generation and acquisition hardware requirements. The CRC method is also capable of instant rapid response measurements as the signal responds in real time without the need to wait for a returning pulse.

1. Introduction

Ultrasonic methods offer a promising approach for industrial in-situ determination of viscosity made from the exterior surface of a component in real time. One particular application is the lubricant viscosity inside a journal bearing. The oil film is subject to temperature, pressure, and shear inconsistencies so the viscosity inside the bearing gap can be significantly different from that in the bulk oil supply. The use of ultrasound to measure tribological parameters has been well documented. Conventional ultrasonic techniques rely on pulsed ultrasound to investigate tribological properties such as lubricant film thickness [1,2], contact stress [3,4], surface wear [5,6], and lubricant properties [7–9].

Mason et al. was the first to highlight the relationship between the shear impedance of a liquid and phase of an ultrasonic wave in 1949 [10]. Whilst techniques still use phase to measure the viscosity of liquid

[11], viscosity can also be correlated to amplitude [7] and frequency change. The Doppler viscometer uses the frequency shift of longitudinal ultrasonic pulses to measure the viscosity of a fluid [12,13] while longitudinal waves have also been combined with shear wave modes to increase the proportion of shear ultrasonic energy incident upon the liquid [14]. The use of surface waves to increase the surface area exposed to the liquid, and also physical additions to ultrasonic apparatus such as the development of wave guides, matching layers and Perspex wedges have all been developed for potential in-situ use [15–17].

Whilst these methods can improve the capability of ultrasonic rheology, practicalities for physical implementation are flawed as many techniques require direct contact between the wave source and liquid. Rich and Roth [18], and Woodward et al. [9] instrumented components, being the first to make viscosity measurements from a counter surface, however the techniques still required liquid immersion. The challenge to measure the shear acoustic impedance of a liquid through

* Corresponding author at: The Leonardo Centre for Tribology, University of Sheffield, Sir Frederick Mappin Building, Mappin Street, Sheffield S13JD, UK.
E-mail address: ofmanfredi@sheffield.ac.uk (O.F. Manfredi).

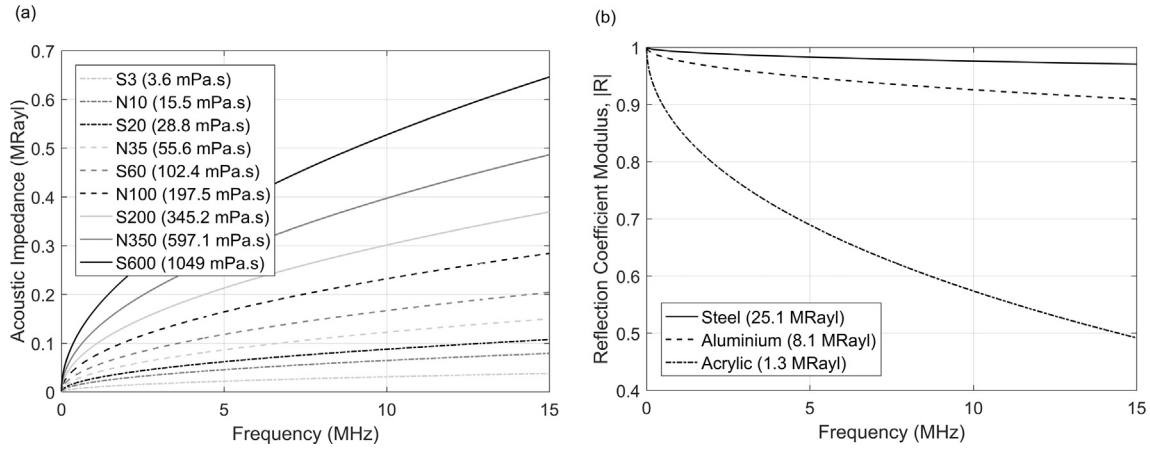


Fig. 1. (a) A simulation of the influence of frequency on the acoustic impedance of liquid at 25 °C (Eq. (6)). (b) A reflection coefficient modulus simulation (Eq. (7)) expected from S200 oil at 345.2 mPa.s with a steel, aluminium and acrylic interface at 25 °C.

a metallic substrate exists due to the high attenuative behaviour of shear waves in liquid. Resonance methods use the influence of the liquid on the phase of the shear wave to relate the time lag of the wave to viscosity, an effect which is amplified by the measurement of multiple reflections using polymeric or silicone delay lines as a wave couplant to the liquid [19,20]. A matching layer can be used to improve ultrasonic viscosity measurement through a metallic component, consisting of a quarter wavelength thick layer of intermediate acoustic impedance material placed between the solid and liquid. The layer acts to increase the proportion of ultrasonic energy incident upon the liquid [7]. Another approach to amplify the sensitivity of ultrasound to a solid-liquid interface is by using a multiple echo approach. The phase shift and amplitude reduction of the ultrasonic wave accumulates with the number of reflections hence a higher order reflection is processed to extract signal features [20,21].

The approach taken in the present work is based on the continuously repeated input of a swept frequency (chirp) shear ultrasonic waveform. The multiple reflections at the liquid interface, and elsewhere in the system, are then superimposed to form a standing wave. The standing wave can then be analysed to determine the viscosity of the liquid at the liquid-solid interface. This has a number of advantages; firstly the approach is rapid (there is no need to wait for the return of repeated reflections), secondly it has the potential for increased sensitivity, and finally the waves can be produced and digitised using low cost hardware. The improved sensitivity means that the technique has the potential for in-line viscometer applications which require viscosity measurement through a metallic interface.

2. Theory: Ultrasonic viscosity measurement

The fundamental laws that govern the reflection coefficient for a single burst of ultrasonic energy also apply to the waves which form a standing wave when they too meet an interface. Hence the following ultrasonic-viscosity equations are correct for each individual wave that contributes to the formation of the standing wave. The standing wave is a superposition of multiple waves, and thus the sum of many boundary interactions, which all contribute to the overall standing wave amplitude spectrum. The relationships outlined in the following equations therefore demonstrate how each single wave used to compose a standing wave is influenced by viscosity, subsequently defining how the standing wave amplitude is governed.

When an ultrasonic shear wave meets a solid-liquid boundary, a proportion of the wave is lost to the liquid and the remainder of the wave is reflected. The proportion reflected is known as the reflection coefficient, R and is described by:

$$R = \left| \frac{z_l - z_s}{z_l + z_s} \right|, \quad (1)$$

where z_s and z_l are the shear acoustic impedance of the solid and liquid respectively. The acoustic impedance of a solid material z_s is a real quantity, defined by the product of the solid density, ρ_s and velocity of shear waves c_s where

$$z_s = \rho_s c_s, \quad (2)$$

The shear acoustic impedance of a liquid z_l , is a complex quantity dependent on the liquid density ρ_l , and complex shear modulus of the liquid, G [22]. Given by

$$z_l = \sqrt{\rho_l G}, \quad (3)$$

where G is the complex variable:

$$G = G' + iG'', \quad (4)$$

where G' is the storage modulus and G'' is the loss modulus. The test samples used in this work were all Newtonian. For the case of a Newtonian liquid, relaxation effects are negligible, thus G' is zero, and G'' is defined by ω the radial frequency ($\omega = 2\pi f$), and dynamic viscosity, η of the oil,

$$G'' = \omega\eta. \quad (5)$$

z_l of a Newtonian liquid can then be expressed by [22]:

$$z_l = \sqrt{i\rho_l\omega\eta} \quad (6)$$

This relationship between η , z_l and ω , (Fig. 1a) indicates greater shear acoustic impedance differences between a range of viscosities at higher frequencies. Based on Fig. 1b, if one intended to increase the acoustic impedance measured for a given liquid, a material with low acoustic impedance itself would be chosen as the substrate and a high frequency shear wave would be required.

Combining Eqs. (3) and (6) into (1) and expressing the reflection coefficient in terms of magnitude gives:

$$|R| = \left| \frac{\sqrt{i\rho_l\omega\eta} - \rho_s c_s}{\sqrt{i\rho_l\omega\eta} + \rho_s c_s} \right|. \quad (7)$$

The reflection coefficient modulus, $|R|$ of the Cannon standard S200 oil is shown in Fig. 1b when calculated at three solid material interfaces (steel, aluminium, and acrylic). The further z_s deviates from z_l , the higher $|R|$ at each frequency. The $|R|$ here has been calculated based on Eq. (1), where z_l is a function of frequency and z_s is 25.1, 8.1 and 1.3 MRayl for steel, aluminium and acrylic respectively. The real part of z_l for S200 oil ranges from 0.00095 MRayl at 100 Hz to 0.36 MRayl at 15 MHz. Thus providing an explanation why liquid viscosity

measurement through a steering part component is difficult.

To overcome this, a ML can be used to increase the influence of viscosity on the reflection coefficient [7]. This is achieved by placing a quarter wavelength thick layer of intermediate acoustic impedance material between the solid and liquid to increase the proportion of ultrasonic energy incident upon the liquid in the configuration shown in Fig. 5a. The ideal acoustic impedance of the layer is defined by:

$$z_m = \sqrt{z_l z_s}. \quad (8)$$

The ML thickness is chosen to be one quarter wavelength of the resonant frequency of the transducer, this is used to create destructive interference of the reflected wave within the layer. For example a 5 MHz centre frequency transducer would require a 50 μm thick ML with the speed of sound equal to 1000 m s^{-1} , as shown by:

$$t_m = \frac{nc_m}{4f}, \quad (9)$$

where t_m and c_m are the thickness and shear speed of sound in the ML respectively, and n is a natural integer. Polyimide is a chemically inert polymer available at the desired thickness with suitable acoustic properties (specified by Eqs. (8) and (9) when matched with aluminium) and so has been used herein. In practice, $|R|$ is measured by the relative amplitude of a reference signal A_r , and measurement signal A_m , when a solid-air interface or a solid-liquid interface is present respectively. $|R|$ can therefore be expressed by:

$$|R| = \frac{A_m}{A_r}. \quad (10)$$

As the complex shear acoustic impedance of a liquid is viscosity dependent, measurement is possible by the relative signal amplitude difference between the solid-air and solid-liquid signals [23].

3. Methodology: Continuously repeated chirp

The CRC methodology has been developed using the principals of standing waves and resonance [24]. The standing wave is produced using a continuously repeating frequency sweep (chirp). The frequency sweep is centred on the resonant frequency of the transducer, and the beginning and end frequencies defined by the frequency sweep span, chosen to lie within the operational bandwidth of the transducer.

The rate of change of frequency of the sweep is considered to be small enough to permit the assumption that, at a given point in the sweep, the change in frequency content of the superimposed reflections that form the standing wave is sufficiently small to allow it to be considered a single frequency. This approach can therefore be described as generating a 'quasi-static' standing wave.

Each reflection from the solid-liquid interface and the transducer-solid interface superimpose along with incident waves to generate a static standing wave of variable frequencies. The resultant standing wave is the sum of multiple reflections at each frequency within the sweep, the amplitude of which is defined for each frequency by the degree of destructive and constructive interference. The repeating linear frequency sweep identifies the resonant frequencies shared by the transducer and component, presented as antinodes.

The signal is composed of nodes and antinodes, their frequency and amplitude depends on the geometry of the component and bandwidth of the transducer, shown schematically in Fig. 2c. The transducers are arranged in a pitch-catch arrangement to permit continual reinforcement of the standing wave, as the excitation signal is continually generated to maintain the standing wave. The second transducer is used to capture the standing wave when a measurement is required. A spectrogram of the digitised received signal shows the linear response of the standing wave amplitude with frequency over the sweep time (Fig. 3).

The technique presented here uses the anti-node frequencies as measurement locations, however this selection is completed post analysis; the signal shown in Fig. 3 is that captured when a measurement is

made. The standing wave reflection coefficient, S at the anti-node, $S_{(pk)}$ is therefore defined by Eq. (11) where $A_{m(pk)}$ is the peak anti-node amplitude in the solid-liquid condition and $A_{r(pk)}$ the peak amplitude of the same anti-node peak in the solid-air condition.

$$S_{(pk)} = \frac{A_{m(pk)}}{A_{r(pk)}} \quad (11)$$

A fundamental feature of a standing wave is the resonant frequency f_s ; each resonant peak is separated by the fundamental harmonic, f_1 , where $f_1 = f_s$. The same order peak of both the reference and measurement signal must be used to find S .

The influence of a liquid on the standing wave can be seen in Fig. 4 as a reduction of the peak amplitude for the solid-liquid interface. By combining the CRC method with the ML approach a resonant peak of the highest sensitivity can be achieved at the frequency which is completely constructive within the component, and completely destructive within the ML. Thus the optimum ML thickness would be $\frac{1}{4}$ wavelength of the highest amplitude resonant peak in a component before the addition of a ML. From Fig. 4b it is clear that multiple resonant frequencies are influenced by the ML. A characteristic reduction in anti-node amplitude with a Cauchy distribution centred on the corresponding resonant frequencies of the component, transducer and ML. Many resonant peaks can be identified, although for the purposes of this paper the resonance found to have the greatest sensitivity following an initial liquid calibration was chosen in each arrangement.

4. Experimental setup

Fig. 5a is a schematic diagram of the measurement apparatus. Four 5 MHz shear ultrasonic transducers (DeL Piezo Specialties LLC) were bonded to the base of a 7.38 mm thick aluminium plate. A pair for the condition without the ML and a pair for measurement with the 50 μm polyimide (DuPont) ML, each arranged in the pitch-catch configuration.

A 9 MHz frequency span was used at a centre frequency of 5 MHz over a 10 ms sweep duration with a 32 ns sample rate. The sweep duration was defined previously, being sufficiently long to achieve amplitude saturation of the standing wave. Ultrasonic signals were amplified and generated using a Kiethly 3390 Arbitrary Waveform Generator (AWG) at a peak to peak voltage of 10 V, and received using a PicoScope 5000a USB oscilloscope. Data was analysed and stored in real time using a PC with an acquisition interface written in LabView. A TC-08 NI device was used with a K-type thermocouple to monitor the component and liquid temperature for all measurements, all of which remained within 1 °C. The experiment is therefore considered to be isothermal, however Kazys et al. [25] discusses issues for a similar measurement which arise as acoustic properties change due to a change in temperature.

Before each test the solid-air interface, (aluminium or ML) was cleaned with isopropanol, left to dry then the reference signal was recorded. The test oil was then deposited on the surface and the standing wave amplitude and temperature acquired for the sample. The test sample was deposited onto the measurement surface using a pipette, an area of 1.5 cm^2 (the same area of the ML in Fig. 5b) was covered in each measurement case, and care was taken to ensure the sample remained within the marked area. Error bars for all data presented were calculated from the standard deviation of five independently repeated experiments, where in each instance three repeats were taken to account for signal fluctuations, producing fifteen measurement signals for each oil in total. Fifteen reference signals were captured in between each oil measurement to provide individual reference data for each oil sample. A Couette Brookfield viscometer was used to validate ultrasonic measurement of nine Cannon standard Newtonian oils used to form a calibration curve.

S_{pk} was determined for the selected peak by taking the Fast Fourier Transform, (FFT) of each signal using LabView. The FFT of the signals

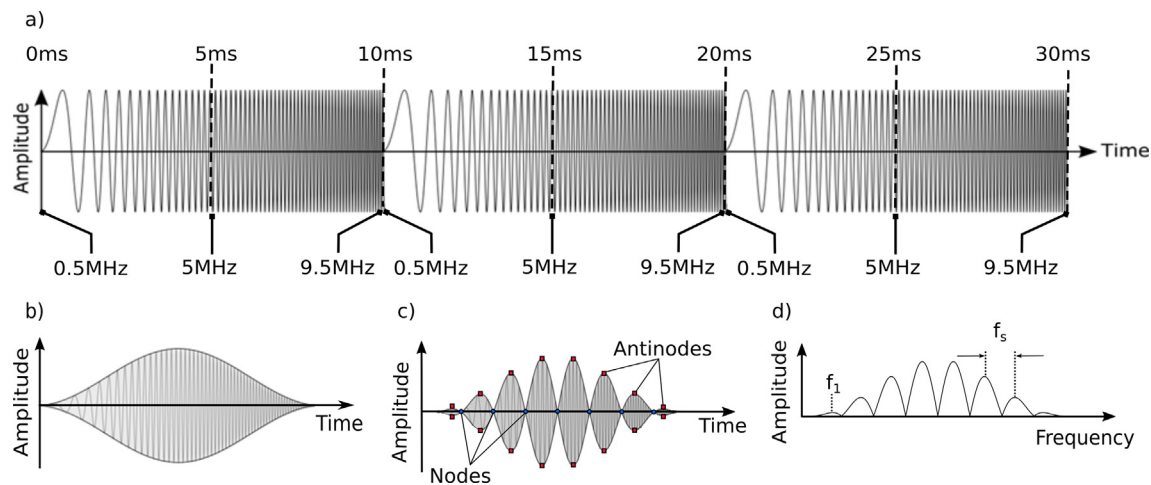


Fig. 2. (a) Schematic illustration of the continuously repeated frequency sweep applied to the generating transducer. (b) A schematic representation of the modulating effect of the transducer on the frequency sweep transmitted into the substrate. (c) A schematic representation of the modulating effect of the component and transducer on the signal amplitude. (d) A schematic FFT of the time domain signal in (c) indicating the first harmonic as f_1 and the resonant frequency f_s .

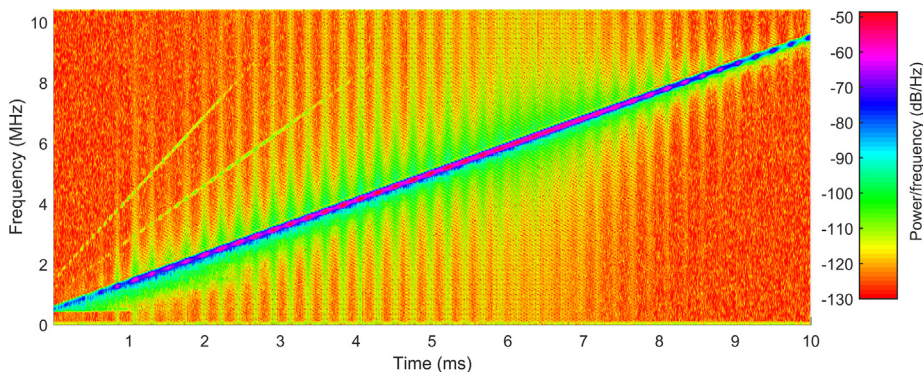


Fig. 3. Spectrogram of a measurement signal using the CRC method, created by the input of a continuously repeating chirp (0.5–9.5 MHz frequency sweep with a 10 ms sweep time). The spectrum shows the standing wave generated within the aluminium component and the variation in amplitude of the standing wave as the time and frequency increase.

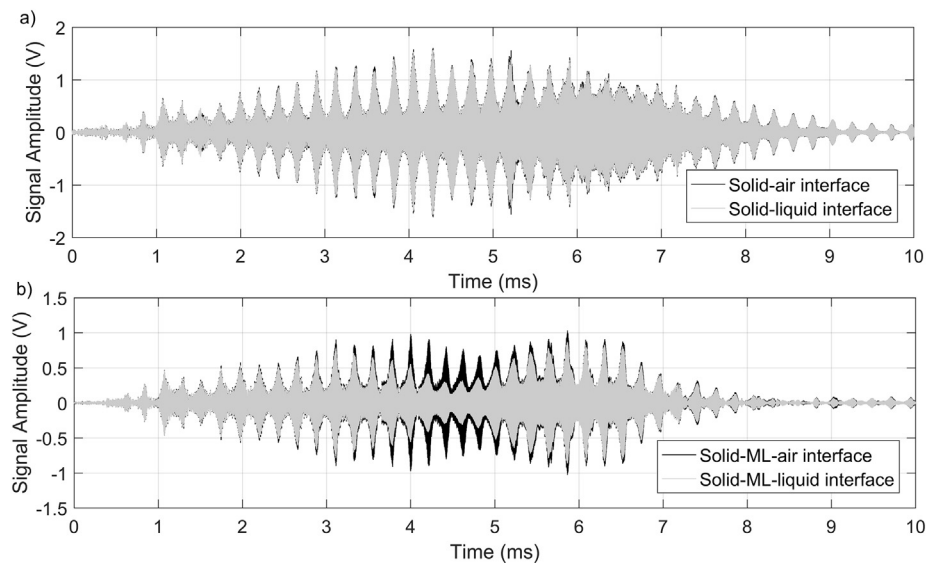


Fig. 4. (a) A time domain CRC signal captured in the solid-air and solid-oil interface conditions. (b) A time domain CRC signal with a ML captured in the solid-air and solid-oil interface conditions.

presented in Fig. 4a and b are those depicted in Fig. 6a and b respectively.

The S value can be calculated at every frequency, shown graphically in Fig. 7 for each calibration oil.

Fluctuation of the S value with frequency indicates the importance

of peak selection. This is due to the fact that the liquid has a greater influence on the amplitude of the antinodes, highlighting the greater sensitivity of the method at these points by lower S values (Fig. 7).

The response of each peak is measured for oils of a range of viscosities to produce a calibration curve. Several resonant frequency

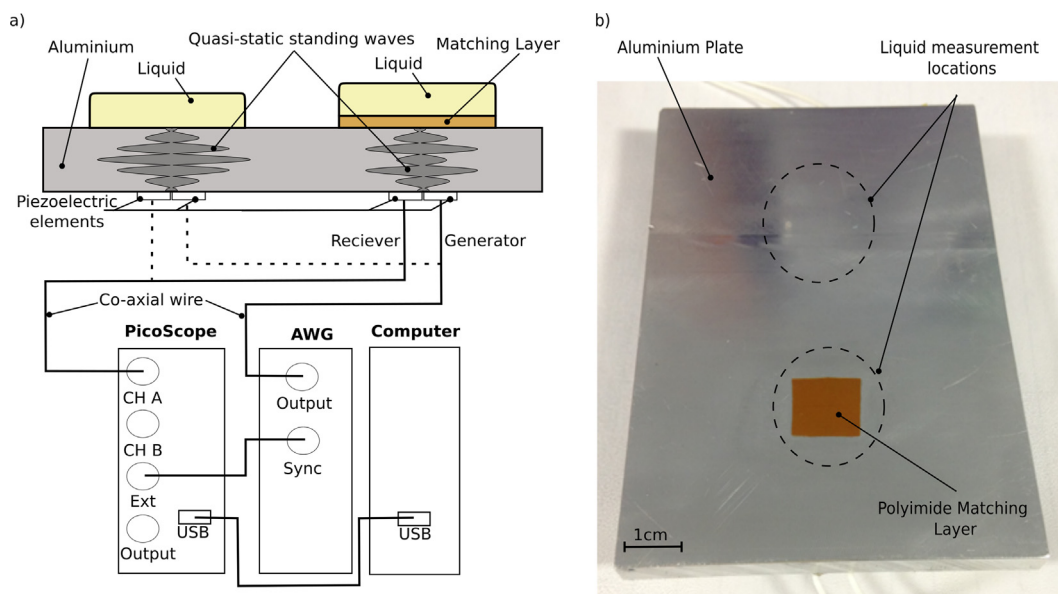


Fig. 5. (a) Schematic illustration of the apparatus and hardware used herein. (b) An image of the aluminium component.

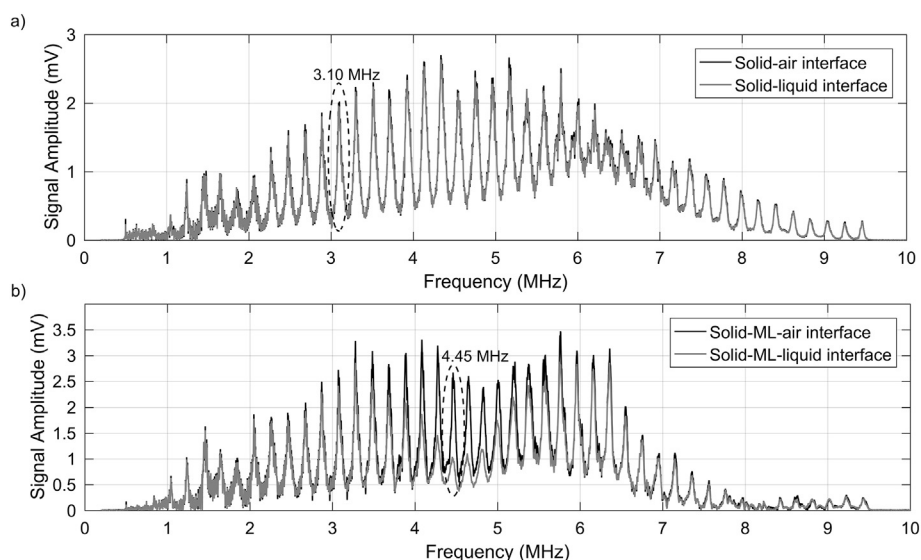


Fig. 6. (a) FFT profile of Fig. 4a, a CRC signal with no ML. (b) The FFT profile of Fig. 4b a CRC signal with the addition of the ML.

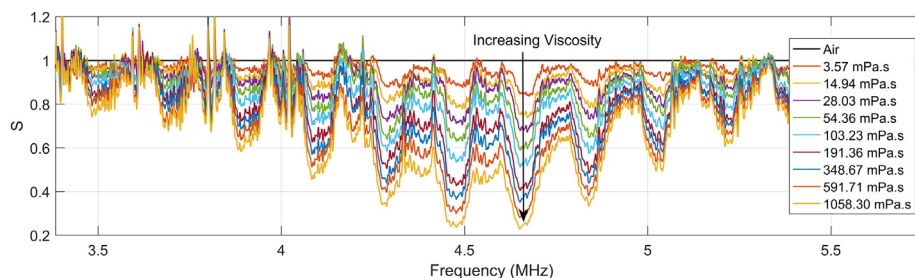


Fig. 7. A figure to show how S varies with frequency for the CRC method with a ML.

responses were analysed to find the resonant peak with the highest sensitivity. With the presence of a ML the 4.45 MHz resonant frequency (Fig. 6b) is shown to have the highest sensitivity to viscosity. The equivalent resonant frequency was not present in the absence of the ML, consequently the resonant peak with the highest variation with viscosity was selected, this being 3.1 MHz. These peaks have been highlighted by elliptical dashed markers in Fig. 6a and b.

5. Test liquid results

Newtonian oils were measured with and without a ML, [Table 1](#) depicts the viscosity and density of the oils tested. The samples were Newtonian mineral hydrocarbon base oils certified by the NIST (National Institute of Standards and Technology) and produced by The Cannon Instrument Company.

Table 1
Density and viscosity of Cannon standard oils at 25 °C.

Cannon standard oil	Density (kg/m ³)	Tabulated viscosity, (Cannon Instrument Company) (mPa s)	Couette viscometer viscosity (mPa s)
S3	0.85	3.66 ± 0.0307	3.57 ± 0.04
N10	0.85	16.19 ± 0.1360	14.94 ± 0.15
S20	0.85	30.19 ± 0.2536	28.03 ± 0.28
N35	0.85	58.65 ± 0.4927	054.36 ± 0.54
S60	0.85	108.69 ± 0.9130	103.23 ± 1.03
N100	0.85	210.70 ± 1.7699	191.36 ± 1.91
S200	0.85	366.17 ± 3.0758	348.67 ± 3.49
N350	0.85	635.24 ± 5.3360	591.71 ± 5.92
S600	0.85	1119.60 ± 9.4046	1058.30 ± 10.58

Fig. 8 shows the calibration curve for CRC results with and without the presence of the ML. The relationship between viscosity and temperature can be best described using the Vogel equation [26], hence this was used to define the viscosity of the oils at the measured temperature using data supplied by the Cannon Instrument Company (Table 1).

The calibration curves shown in Fig. 8 are in the exponential form as they follow the mathematical relationship outlined in Eq. (7). The coefficient of determination for Eqs. (12) and (13) are 0.960 and 0.999 without, and with a ML respectively.

$$\eta = 1.448 \times 10^{31} \exp(-68.78S) \quad (12)$$

$$\eta = 8416 \exp(-8.189S) \quad (13)$$

The equations of these relationships along with the coefficient of determination values were calculated from the mean peak amplitude of the antinode at 3.1 and 4.45 MHz for results without and with a ML respectively.

6. Blended oil measurement results

In order to test the experimental capability of each method, oil blends were produced using a mixture of two Cannon standard oils. The samples were blended by initial mechanical stirring, followed by placement in an ultrasonic bath for 20 min at room temperature. A sufficiently long time was left before testing to ensure settling of any air or vapour bubbles. The uniformity of each blended oil was assessed by the samples visual appearance to ensure no difference in colour or layer could be seen within the blend. Compositions and measured Couette viscosity values of the blended oils can be found in Table 2.

Table 2
S600:S200 and S600:S3 blended Cannon standard Newtonian viscosity oils measured using a Couette rotational viscometer (1% error).

High viscosity band		Low viscosity band	
Oil blend with S600 S200 (%)	Couette viscosity (mPa.s) 24 °C	Oil blend with S600 S3 (%)	Couette viscosity (mPa.s) 24 °C
7.1	1080.1 ± 10.80	42.9	65.1 ± 0.65
14.3	930.1 ± 9.30	50.0	42.0 ± 0.42
21.4	980.2 ± 9.80	57.1	28.3 ± 0.28
28.6	787.4 ± 7.87	64.3	19.4 ± 0.19
35.7	736.0 ± 7.36	71.4	13.5 ± 0.14
42.9	665.0 ± 6.65	78.6	9.3 ± 0.09
50.0	661.1 ± 6.61	85.7	6.7 ± 0.07
57.1	534.9 ± 5.35	–	–
64.3	559.8 ± 5.60	–	–
71.4	468.0 ± 4.68	–	–

The value of S for each blended oil was calculated then converted to viscosity using Eqs. (12) or (13). The ultrasonic viscosity was then evaluated against Couette results to highlight the viscosity band capability of each method. The oils were separated into the low category (0–70 mPa s) and high category (400–1100 mPa s). Fig. 9a and b show the CRC ultrasonic viscosity measurements of the blended oils compared to Couette results. This agreement is improved by the addition of the ML, results of which are shown in Fig. 10a and b.

As predicted, the ML gives results with smaller errors and superior agreement with Couette viscosity results. The addition of a ML, as outlined in [7] significantly improves in-situ liquid measurements through a metallic substrate. ΔS is 13 times higher with the addition of a ML, increasing the range of measurements between 0 and 1000 mPa s from 0.056 to 0.73, calculated using Eqs. (12) and (13). The deviation of ultrasonic viscosity from perfect agreement in Fig. 10a is likely to be caused by poorness of fit to the calibration curve (Fig. 8) seen in the region of 20–70 mPa s; if this effect was a result of non-Newtonian effects one would expect this deviation to be present at higher viscosities also in which it is not (Fig. 10b).

The lowest errors and thus highest accuracies are achieved using the ML in combination with the CRC method, shown to reduce errors by an order of magnitude. Measurement noise may be reduced by increasing the number of samples and excitation voltage, thus the data presented here must not be considered as the limit of each technique, rather a comparison of the ultrasonic viscosity measurement results.

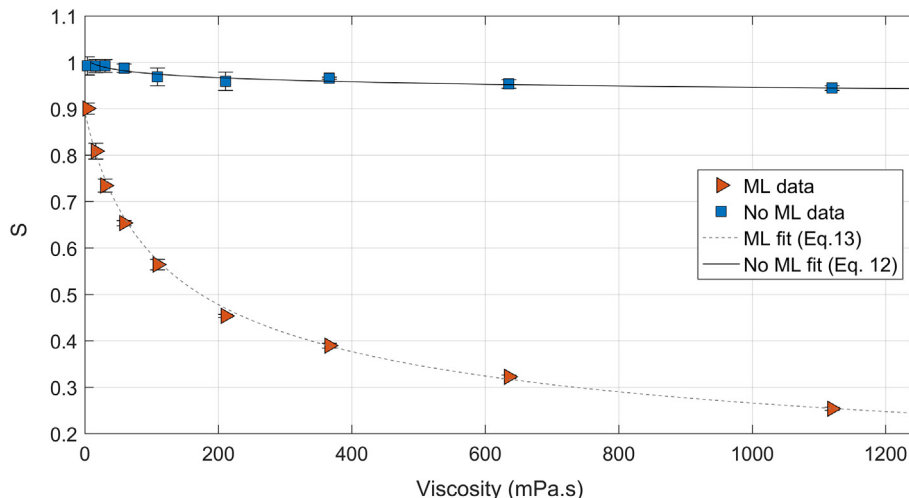


Fig. 8. Calibration curves produced using the CRC method with and without the ML.

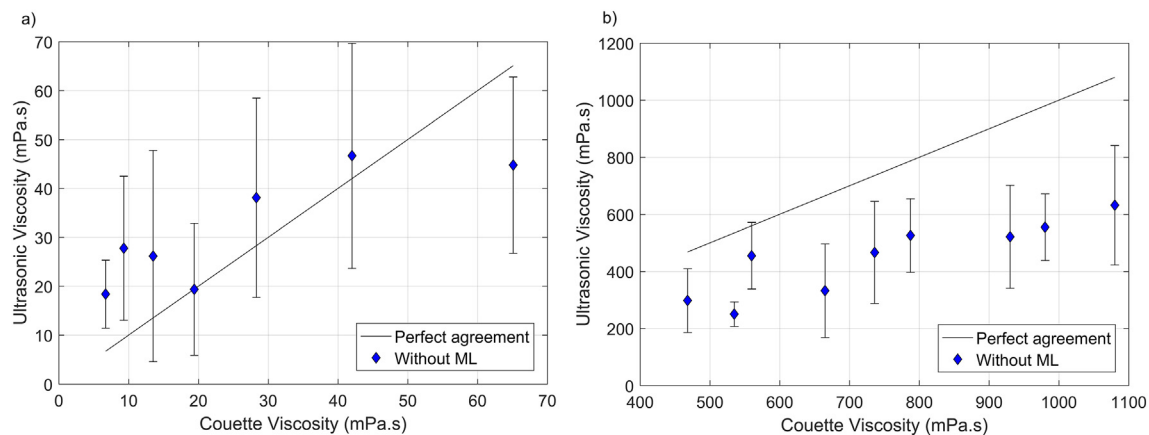


Fig. 9. (a) and (b) Ultrasonic measurement versus a Couette viscosity measurements for each blended oil without a ML.

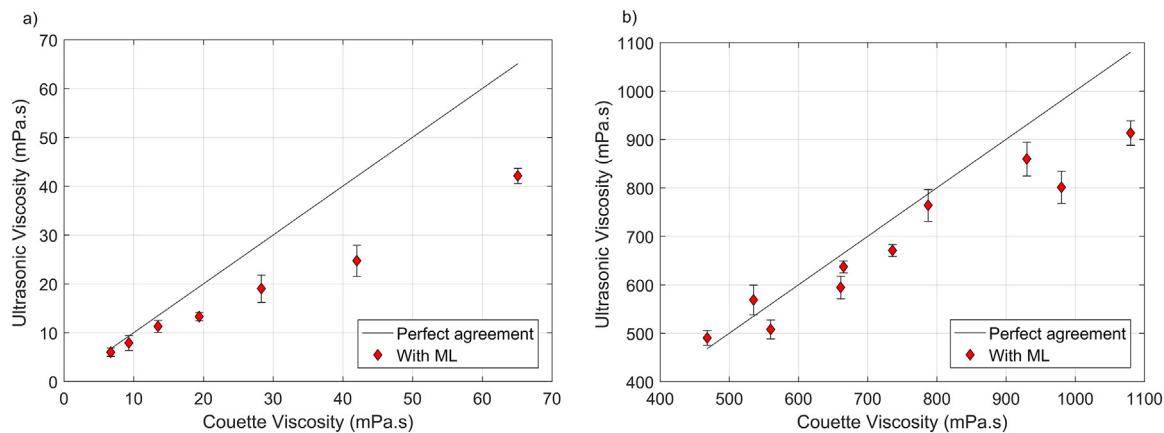


Fig. 10. (a) and (b) Ultrasonic measurement versus a Couette viscosity measurements for each blended oil with a ML.

7. Discussion

To realise the quasi-static standing wave method as a capable tool for Newtonian viscosity measurement through a metallic substrate, the ability to predict the viscosity of an unknown liquid after a calibration process has been evaluated. As demonstrated by Camara et al. [20] the influence of phase increases with the number of reflections within a structure. The principals of standing waves adopted here take advantage of this by acquiring a signal which is a result of several reflections, presenting itself as a change in standing wave amplitude. The complex liquid acoustic impedance is measured by a comparison of the standing wave amplitude of an antinode in a solid-air and a solid-liquid condition.

As shown in Figs. 9 and 10, the ability of the CRC method is greatly improved by the addition of an acoustic matching layer in between the measurement fluid and aluminium component. While the matching layer produces a significant sensitivity and accuracy rise and has been shown to be practically viable for in-situ measurement, the standing wave method alone (without a ML) could potentially provide a low cost alternative for real-time viscosity measurement in a higher viscosity band (> 400 mPa.s) [27,7]. This may be useful where it is not possible to insert a matching layer on the contact surface in a bearing for example.

Pulsing systems used for burst capture methods need relatively complex operating systems as signal generation requires sample rates of 2–5 times greater than the frequency of interest. For example a system would need a sample rate of 20–50 MHz to generate a 10 MHz pulse. In order to sufficiently resolve comparable digitisation rates, 50–100 MHz would be required in order to adequately resolve the signal. To profile

viscosity over short periods of time the burst sine wave method allows a short time interaction with liquids with the pulse length in the order of μ s, rather than ms in the case of the CRC method.

The CRC method uses a long duration swept frequency excitation signal, many low cost direct digital synthesis techniques are available to produce continuous wave signals. The generation of a standing wave within the component concedes the RMS of the signal is sufficient to produce a measurement. Unlike pulsed methods the digitisation rate of the acquisition is controlled by the sweep time rather than the frequency of the standing wave. This makes it possible to reduce the acquisition sample rate to 100s or even 10s of kHz, simplifying the acquisition hardware substantially.

8. Conclusions

This work presents the use of a continuously repeated chirp input to generate a quasi-static standing wave at a solid-liquid interface for the purpose of measuring liquid viscosity. This has the effect of amplifying the reflection coefficient at an acoustically mismatched liquid- metallic interface. The method improves the sensitivity over a conventional pulsed wave method. Optimisation of the CRC technique can produce an acceptable sensitivity of viscosity measurement for viscosities > 400 mPa.s. Implementation of a matching layer has also been evaluated, improving sensitivity by 13 times. The CRC method requires low cost signal generation and acquisition hardware, while also maintaining the ability to produce instantaneous very quick measurement. For some cases where viscosity is high, the CRC method alone, without the matching layer, can provide sufficient accuracy for Newtonian viscosity measurement in-situ.

9. Declarations of interest

None.

Acknowledgements

This work was supported by the Engineering and Physical Sciences Research Council (EPSRC) with funding through the Centre for Doctoral Training in Tribology (Manfredi), and the Fellowship in Tribo-Acoustic Sensors (Dwyer-Joyce and Schirru).

Appendix A. Supplementary material

Supplementary data associated with this article can be found, in the online version, at <https://doi.org/10.1016/j.ultras.2018.08.002>.

References

- [1] R.S. Mills, E. Avan, R.S. Dwyer-Joyce, Piezoelectric sensors to monitor lubricant film thickness at piston-cylinder contacts in a fired engine, *Proc. Inst. Mech. Eng. Part J. J. Eng. Tribol.* 227 (2012) 100–111, <https://doi.org/10.1177/1350650112464833>.
- [2] R.S. Dwyer-Joyce, P. Harper, B.W. Drinkwater, A method for the measurement of hydrodynamic oil films using ultrasonic reflection, *Tribol. Lett.* 17 (2004) 337–348.
- [3] M.B. Marshall, R. Lewis, B.W. Drinkwater, R.S. Dwyer-Joyce, An ultrasonic approach for contact stress mapping in machine joints and concentrated contacts, *J. Strain Anal. Eng. Des.* 39 (2004) 339–350, <https://doi.org/10.1243/0309324041223971>.
- [4] M.B. Marshall, R. Lewis, S. Björklund, Experimental characterization of wheel-rail contact patch, *J. Tribol.* 128 (2006) 493–504, <https://doi.org/10.1115/1.2197523>.
- [5] H. Brunskill, P. Harper, R. Lewis, The real-time measurement of wear using ultrasonic reflectometry, *Wear* 332–333 (2015) 1129–1133, <https://doi.org/10.1016/j.wear.2015.02.049>.
- [6] A.S. Birring, H. Kwun, Ultrasonic measurement of wear, *Tribol. Int.* 22 (1989) 33–37, [https://doi.org/10.1016/0301-679X\(89\)90006-6](https://doi.org/10.1016/0301-679X(89)90006-6).
- [7] M.M. Schirru, R.S. Mills, R.S. Dwyer-Joyce, O. Smith, M. Sutton, Viscosity measurement in a lubricant film using an ultrasonically resonating matching layer, *Tribol. Lett.* 60 (2015) 1–11, <https://doi.org/10.1007/s11249-015-0619-x>.
- [8] M.S. Greenwood, J.A. Bamberger, Measurement of viscosity and shear wave velocity of a liquid or slurry for on-line process control, *Ultrasonics* 39 (2002) 623–630, [https://doi.org/10.1016/S0041-624X\(02\)00372-4](https://doi.org/10.1016/S0041-624X(02)00372-4).
- [9] J.G. Woodward, A vibrating-plate viscometer, *J. Acoust. Soc. Am.* 25 (1953) 481–491.
- [10] W.P. Mason, W.O. Baker, H.J. McSkimin, J.H. Heiss, Measurement of shear elasticity and viscosity of liquids at ultrasonic frequencies, *Phys. Rev.* 75 (1949) 936–946.
- [11] V.V. Shah, K. Balasubramaniam, Measuring Newtonian viscosity from the phase of reflected ultrasonic shear wave, *Ultrasonics* 38 (2000) 921–927.
- [12] J. Wiklund, B. Birkhofer, S. Ricci, R. Haldenwang, M. Stading, Flow-Viz – a fully integrated and commercial in-line fluid characterization system for industrial applications, 9th Int. Symp. Ultrason. Doppler Methods Fluid Mech. Fluid Eng. (2014) 165–168.
- [13] D.M. Pfund, M.S. Greenwood, J.A. Bamberger, R.A. Pappas, Inline ultrasonic rheometry by pulsed Doppler, *Ultrasonics* 44 (2006) 477–482, <https://doi.org/10.1016/j.ultras.2006.05.027>.
- [14] S.H. Sheen, H.T. Chien, A.C. Raptis, Ultrasonic Methods for Measuring Liquid Viscosity and Volume Percent of Solids, Energy Technology Division, U.S. Department of Energy, 1997.
- [15] P. Kielczyński, M. Szalewski, A. Balcerzak, A.J. Rostocki, Measurements of the viscosity of liquids in function of pressure and temperature using SH surface acoustic waves, *IEEE Int. Ultrason. Symp. IUS* (2011) 535–538, <https://doi.org/10.1109/ULTSYM.2011.0129>.
- [16] A. Turtton, D. Bhattacharyya, D. Wood, Liquid density analysis of sucrose and alcoholic beverages using polyimide guided Love-mode acoustic wave sensors, *Meas. Sci. Technol.* 17 (2005) 257–263, <https://doi.org/10.1088/0957-0233/17/2/005>.
- [17] R. Kazys, R. Sliteris, R. Raisutis, E. Zukauskas, A. Vladisauskas, L. Mazeika, Waveguide sensor for measurement of viscosity of highly viscous fluids, *Appl. Phys. Lett.* 103 (2013) 204102-1–204102-4, <https://doi.org/10.1063/1.4829639>.
- [18] W. Roth, S.R. Rich, A. New, Method for continuous viscosity measurement. General theory of the ultra-viscoson, *J. Appl. Phys.* 24 (1953) 940, <https://doi.org/10.1063/1.1721406>.
- [19] M.S. Greenwood, J.D. Adamson, L.J. Bond, Measurement of the viscosity-density product using multiple reflections of ultrasonic shear horizontal waves, *Ultrasonics* 44 (2006) 1031–1036, <https://doi.org/10.1016/j.ultras.2006.05.093>.
- [20] V.C. Camara, D. Laux, O. Arnould, Enhanced multiple ultrasonic shear reflection method for the determination of high frequency viscoelastic properties, *Ultrasonics* 50 (2010) 710–715, <https://doi.org/10.1016/j.ultras.2010.02.007>.
- [21] J. Gasparoux, D. Laux, J.Y. Ferrandis, J. Attal, P. Tordjeman, Large frequency bands viscoelastic properties of honey, *J. Nonnewton. Fluid Mech.* 153 (2008) 46–52, <https://doi.org/10.1016/j.jnnfm.2007.11.007>.
- [22] E.E. Franco, J.C. Adamowski, F. Buiocchi, Ultrasonic viscosity measurement using the shear-wave reflection coefficient with a novel signal processing technique, *IEEE Trans. Ultrason. Ferroelectr. Freq. Control.* 57 (2010) 1133–1139, <https://doi.org/10.1109/TUFFC.2010.1524>.
- [23] V. Buckin, E. Kudryashov, Ultrasonic shear wave rheology of weak particle gels, *Adv. Colloid Interf. Sci.* 89 (2001) 401–422.
- [24] R.S. Mills, R.S. Dwyer-Joyce, M.B. Marshall, Continuous Wave Ultrasound for Analysis of a Surface, Patent Application Number 1522677.2., 2017.
- [25] R. Kazys, R. Sliteris, R. Rekuvienė, E. Zukauskas, L. Mazeika, Ultrasonic technique for density measurement of liquids in extreme conditions, *Sensors (Switzerland)* 15 (2015) 19393–19415, <https://doi.org/10.3390/s150819393>.
- [26] R.F. Crouch, A. Cameron, Viscosity-temperature equations for lubricants, *J. Inst. Pet.* 47 (1961) 307–313.
- [27] M.M. Schirru, R.S. Dwyer-Joyce, A model for the reflection of shear ultrasonic waves at a thin liquid film and its application to viscometry in a journal bearing, *Proc. Inst. Mech. Eng. Part J. J. Eng. Tribol.* 230 (2015) 667–679, <https://doi.org/10.1177/1350650115610357>.